Appl. Phys. A (2016) 122:477
DOI 10.1007/s00339-016-0022-y

Applied Physics A
Materials Science & Processing

Sliding wear behavior of laser-nitrided and thermal oxidation-treated Ti–5Al–5Mo–5V–1Cr–1Fe alloy fabricated by laser melting deposition

L. Liu[1] · Y. J. Shangguan[1] · H. Z. Li[1] · H. B. Tang[2] · H. M. Wang[2]

Received: 24 January 2016 / Accepted: 23 March 2016 / Published online: 31 March 2016

Abstract Sliding wear behavior of laser-nitrided and thermal oxidation-treated Ti–5Al–5Mo–5V–1Cr–1Fe (TC18) alloy fabricated by laser melting deposition (LMD) has been investigated to improve on wear resistance of laser melting deposited titanium alloy. The microstructure, wear morphology, hardness and wear rate were examined for the unmodified, laser-nitrided and thermal oxidation-treated LMD Ti–5Al–5Mo–5V–1Cr–1Fe alloy. As compared to α/β basket weave microstructure with fine lamellar α (hcp) observed on the unmodified LMD Ti–5Al–5Mo–5V–1Cr–1Fe alloy, Ti, Ti_2N and TiN were formed on the LMD specimens after laser nitriding. After thermal oxidation, a surface layer composed of rutile TiO_2 was formed on the LMD specimens along with coarsening of α lath. The increase in hardness and wear resistance of the laser-nitrided LMD Ti–5Al–5Mo–5V–1Cr–1Fe alloy is attributed to hard dendritic TiN formed on the specimens. The wear rate of the thermal oxidation-treated LMD specimens was <1 % of that of the unmodified LMD specimens when hardness of the former was twice as much as the latter. The superior sliding wear resistance of the thermal oxidation-treated LMD specimens is attributed to the presence of the lubricious rutile oxide layer and hardened diffusion zone.

✉ L. Liu
liulin@cumtb.edu.cn

[1] School of Mechanical and Electrical Engineering, China University of Mining and Technology (Beijing), D11 Xue Yuan Lu, Beijing 100083, China

[2] Engineering Research Center of Ministry of Education on Laser Direct Manufacturing for Large Metallic Components, Beihang University, No. 37 Xue Yuan Lu, Beijing 100191, China

1 Introduction

Recently, laser melting deposition (LMD) undergoes rapid development in fabricating titanium alloy aerospace components [1, 2]. Unlike traditional manufacturing methods such as casting, laser melting deposition produces full density near-net-shape components from powder with shorter manufacturing cycle and higher material utilization rate where no forming equipment is necessary. TC18 titanium alloy with the nominal composition of Ti–5Al–5Mo–5V–1Cr–1Fe alloy is a near β-type titanium alloy which is superior as aircraft structural material [3]. With high strength after annealing among existing titanium alloys, it has excellent long-term work performance below 350 °C ($\leq$10,000 h) [4]. Apart from their attractive mechanical properties, however, titanium alloys generally suffer from poor wear resistance [5]. As compared to extensive research performed on the microstructure and properties of Ti–5Al–5Mo–5V–1Cr–1Fe alloy, little attention has been paid to the sliding wear behavior of laser melting deposited Ti–5Al–5Mo–5V–1Cr–1Fe alloy. It is likely that some form of surface engineering may be exploited to render protection against wear damage for LMD Ti–5Al–5Mo–5V–1Cr–1Fe alloy.

Laser nitriding is a popular way to improve the wear and corrosion performance of titanium alloys. After laser nitriding, a hard composite layer with low friction coefficient is generally obtained after solidification [6]. The microstructure varies with processing parameters and normally comprises of fine nitride needles or dendrites embedded in a nitrogen-rich titanium matrix [7]. Thermal oxidation (TO) treatment from a tribological aspect is another way to improve wear resistance of titanium alloys. Ceramic coatings formed during controlled oxidation, mainly rutile, can offer thick, highly crystalline oxide films

to impart beneficial wear resistance to titanium alloy. Wang et al. [8] and Guleryuz and Cimenoglu [9] investigated the thermal oxidation process for Ti6Al4V and yielded a surface with a low friction coefficient, low wear rate and high load-bearing capacity. Kumar reported that thermal oxidation of titanium at a high temperature above 800 °C and extended period of time, however, would lead to spallation of the oxide layer in spite of the thickness [10]. In this paper, laser nitriding and TO treatment were performed on LMD Ti–5Al–5Mo–5V–1Cr–1Fe alloy, and the microstructure, wear scar and debris of the unmodified, laser-nitrided and TO-treated LMD specimens were examined along with the wear rate, hardness and friction coefficient to investigate their sliding wear behavior.

2 Materials and methods

2.1 Material

Atomized Ti–5Al–5Mo–5V–1Cr–1Fe alloy powder (Haibao Special Metal Materials Co.) was used for laser melting deposition on a LMD system with 8 kW continuous-wave CO_2 laser. The composition of the powder is as follows: 5.5 % Al, 4.82 % Mo, 4.82 % V, 1.02 % Cr, 1.05 % Fe, 0.024 % C, 0.021 % N, 0.10 % O, 0.0028 % H (in wt%) and Ti as the remainder. During LMD, parameters such as laser power of 3 kW, beam diameter of 4 mm and scanning speed of 300 mm/min were used and duplex annealing treatment was performed on the as-deposited specimens. Laser nitriding was conducted on the annealed LMD specimens using laser power of 3.5 kW, beam diameter of 5 mm and scanning speed of 300 mm/min on Rofin DC50 CO_2 laser. Argon was used to purge the air in the chamber until oxygen was less than 80 ppm after which the inlet gas was switched to nitrogen (4 MPa) for laser nitriding. Thermal oxidation treatment was performed on the annealed LMD specimens in aGSL-1700X tube furnace (Hefei Kejing Materials Technology) at 650 °C under a gas mixture of oxygen (80 %) and nitrogen at a flow rate of 150 cc/min. Heating rate of 10 °C/min and holding time of 48 h were used with furnace cooling to room temperature.

2.2 Tribological testing and characterization

The friction coefficients of the specimens sliding against the AISI 52100 bearing steel (conforming to ASTM A295) were measured on a M200 tester (Alfred J. Amsler & Co) using a loading force of 200N with test speed of 200 rd/min for 15 min. Dimension of the specimen was 10 mm × 10 mm × 15 mm, and the test geometry is block-on-wheel. The specimens were cut from the plates of the unmodified, laser-nitrided and TO-treated LMD Ti–5Al–5Mo–5V–1Cr–1Fe alloy, respectively, and smoothened using 1500-grit sandpaper. Inside and outside diameters of the mating ring were 16 and 40 mm, and thickness is 10 mm. Three specimens were tested under each condition, and the average value was recorded. The morphology of the wear scar and debris was observed on scanning electron microscope (JEOL JSM-6510A), and elemental analysis was performed using energy-dispersive spectroscopy (EDS). The microstructure of the specimens was characterized using Rigaku DMax-RB X-ray diffractometer (XRD). Microhardness measurements were made on the polished cross sections of the specimens using an HV-1000 microhardness tester (Shanghai Aolong Xingdi Testing Equipment Co.) with a Vickers indenter and a load of 2 N. The distance between every two indentations was three times longer than the indentation diagonal in order to eliminate the stress field effect near the indentation. The microhardness values reported in this paper are the average values from three specimens.

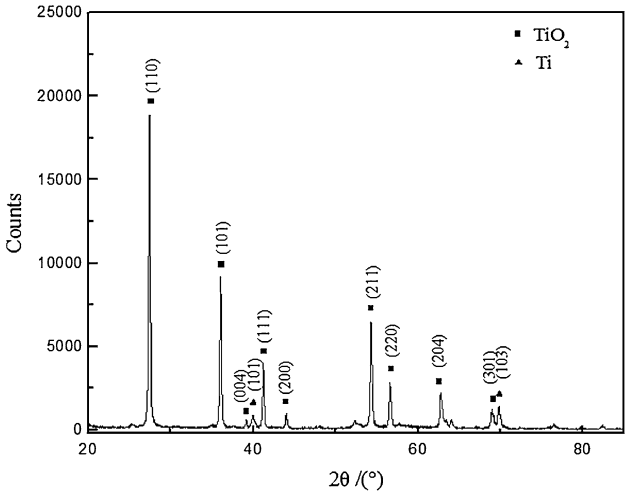

Fig. 1 XRD result of thermal oxidation-treated LMD Ti–5Al–5Mo–5V–1Cr–1Fe alloy

3 Results and discussion

3.1 Microstructure

Unmodified LMD Ti–5Al–5Mo–5V–1Cr–1Fe alloy mainly consisted of Ti, and some Ti_2O was formed because Ti–5Al–5Mo–5V–1Cr–1Fe alloy is active. Apart from Ti, Ti_2N and TiN that were reaction products derived from laser nitriding were observed on laser-nitrided specimens as in our earlier study on fretting wear of laser-nitrided LMD Ti–5Al–5Mo–5V–1Cr–1Fe alloy [11]. Ti and rutile TiO_2 were formed on TO-treated LMD Ti–5Al–5Mo–5V–1Cr–1Fe alloy as shown in Fig. 1 because thermal

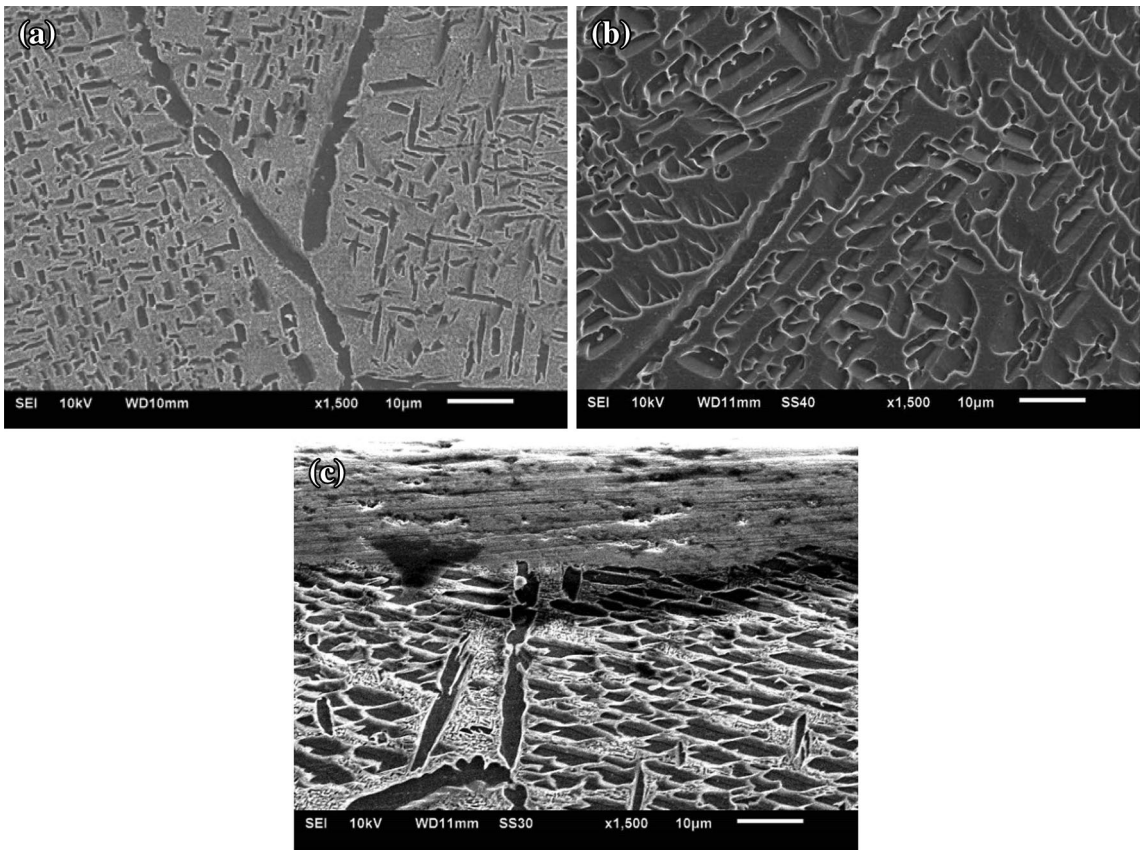

Fig. 2 Scanning electron micrograph of microstructure of: **a** unmodified LMD Ti–5Al–5Mo–5V–1Cr–1Fe alloy, **b** laser-nitrided and **c** thermal oxidation-treated LMD Ti–5Al–5Mo–5V–1Cr–1Fe alloy

oxidation under high oxygen content at elevated temperatures facilitated transformation of metastable Ti_2O to rutile TiO_2 on the surface of specimens. Metallographic observation in Fig. 2a, b reveals α/β basket weave microstructure on the unmodified and laser-nitrided LMD Ti–5Al–5Mo–5V–1Cr–1Fe alloy. Figure 2a shows that fine lamellar α (hcp) growing in many directions was formed due to rapid cooling rate used during laser melting deposition. The aspect ratio of the α colonies, an average of the length of α lath divided by its width, is 3.4. After laser nitriding, denser microstructure was observed (see Fig. 2b). After TO treatment, coarsening of primary α phase due to diffusion was observed where the aspect ratio of α lath decreased to 2.5. As evidenced by the X-ray diffraction results, a thick crystalline rutile surface oxide layer was formed on the thermally oxidized specimen (see Fig. 2c).

3.2 Wear scar and debris morphology

The morphologies of the wear scar and debris are depicted in Figs. 3 and 4, respectively. The tested surface of the unmodified LMD Ti–5Al–5Mo–5V–1Cr–1Fe alloy was identified with plowing grooves, fracture and craters along with some attached micro-cutting chip. A mixture of plate, flake and cutting chip-like debris was observed after sliding wear of the unmodified LMD Ti–5Al–5Mo–5V–1Cr–1Fe alloy. EDS analysis of the plate-like debris in Fig. 4 reveals the preferential transfer of the unmodified LMD Ti–5Al–5Mo–5V–1Cr–1Fe alloy onto the steel mating ring, which is attributed to repeated plastic deformation and plowing adjacent to the contacting surface. The worn surface of laser-nitrided LMD Ti–5Al–5Mo–5V–1Cr–1Fe alloy was characterized by some island-like plateaus dispersed onto plowing streaks. In general, the flake-like wear debris observed on laser-nitrided LMD Ti–5Al–5Mo–5V–1Cr–1Fe alloy was smaller than that obtained on the unmodified LMD Ti–5Al–5Mo–5V–1Cr–1Fe alloy. Besides, a few spherical wear debris particles were observed (see Fig. 4d), and EDS analysis reveals that they are composed of Ti–5Al–5Mo–5V–1Cr–1Fe alloy. It indicates that during dry sliding, frictional heating under repeated high contact stress between the hard dendritic TiN and bearing steel contacting surfaces invoked remelting of fragmented fine Ti–5Al–5Mo–5V–1Cr–1Fe alloy wear debris and ensuing detachment. Figure 3e reveals material pileup along both sides of the wear track on thermal oxidation-treated Ti–5Al–5Mo–

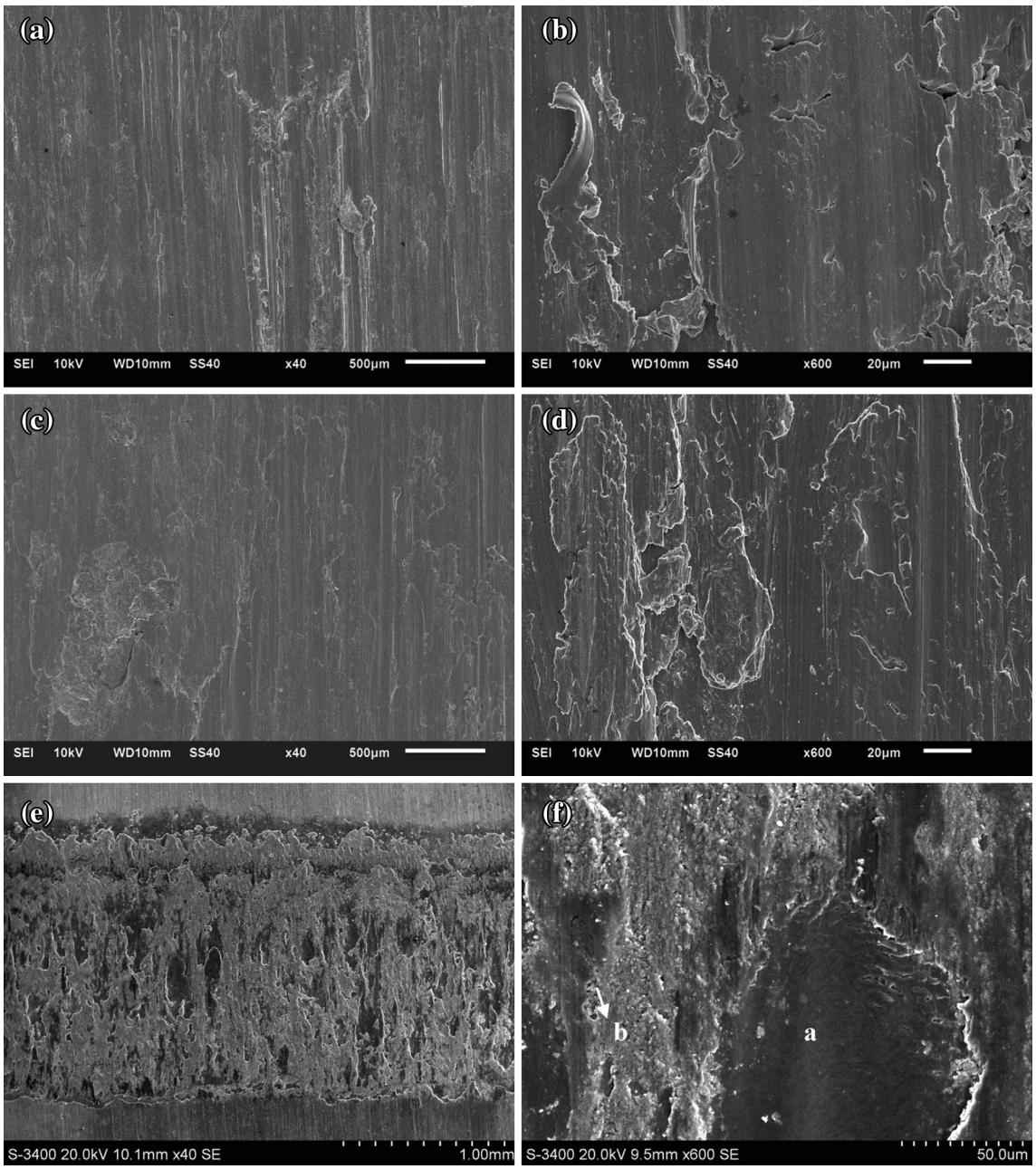

Fig. 3 Scanning electron micrograph of wear scar: **a** low magnification and **b** high magnification of unmodified LMD Ti–5Al–5Mo–5V–1Cr–1Fe alloy, **c** low magnification and **d** high magnification of laser-nitrided Ti–5Al–5Mo–5V–1Cr–1Fe alloy and **e** low magnification and **f** high magnification of thermal oxidation-treated LMD Ti–5Al–5Mo–5V–1Cr–1Fe alloy

5V–1Cr–1Fe alloy. Some streaks parallel to the sliding direction were observed in the center of the worn surface that was covered with a thin layer of irregular fine wear debris particles. The area of the wear scar on the thermal oxidation-treated LMD specimens was reduced significantly as compared to that of the unmodified and laser-nitrided LMD specimens, which indicates superior sliding wear resistance. EDS analysis of the wear scar reveals the presence of Ti–5Al–5Mo–5V–1Cr–1Fe alloy in the crater of the thermal oxidation-treated specimens (area a), while the bright area within or along both sides of the wear track as shown in region b is highly enriched in Fe and O, indicating that they were transferred from the steel mating ring during the sliding wear. As shown in Fig. 4e, f, the wear debris of the thermal oxidation-treated LMD Ti–5Al–5Mo–5V–1Cr–1Fe alloy consists of powder-like fine debris and irregular chunks of powder agglomerates, which indicates tribochemical reaction products. EDS analysis reveals

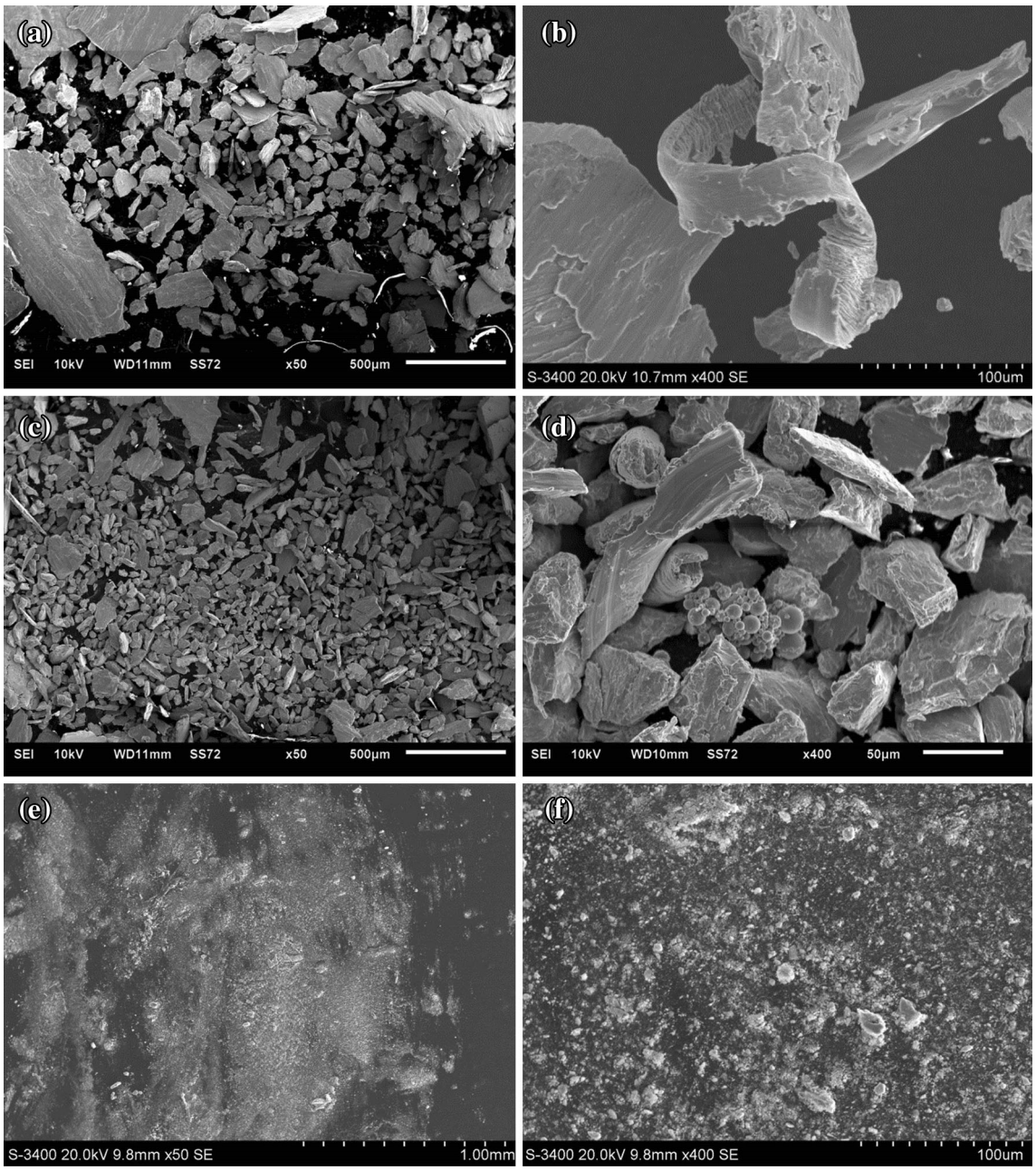

Fig. 4 Scanning electron micrograph of wear debris: **a** low magnification and **b** high magnification of unmodified LMD Ti–5Al–5Mo–5V–1Cr–1Fe alloy, **c** low magnification and **d** high magnification of laser-nitrided Ti–5Al–5Mo–5V–1Cr–1Fe alloy and **e** low magnification and **f** high magnification of thermal oxidation-treated LMD Ti–5Al–5Mo–5V–1Cr–1Fe alloy

that the wear debris is highly enriched in Fe and O, probably originating from iron oxides formed on the steel mating ring due to oxidization under cycling stress and frictional heating during dry sliding. Since a surface layer of angular TiO_2 crystals was formed on the thermal oxidation-treated LMD Ti–5Al–5Mo–5V–1Cr–1Fe alloy which rendered a pair of ceramic/steel contacting surfaces when it slid against the bearing steel, the transfer of steel onto the worn Ti–5Al–5Mo–5V–1Cr–1Fe alloy surface might come from plowing of TiO_2 on the mating ring rather than adhesion.

The microstructure of the unmodified, laser-nitrided and thermal oxidation-treated LMD Ti–5Al–5Mo–5V–1Cr–1Fe alloy after wear is shown in Fig. 5. For the unmodified LMD Ti–5Al–5Mo–5V–1Cr–1Fe alloy, the worn surface was rough and a few tearing open pits were observed on the worn specimen. Plastic deformation in response to repeated high contact stress against the mating surfaces was

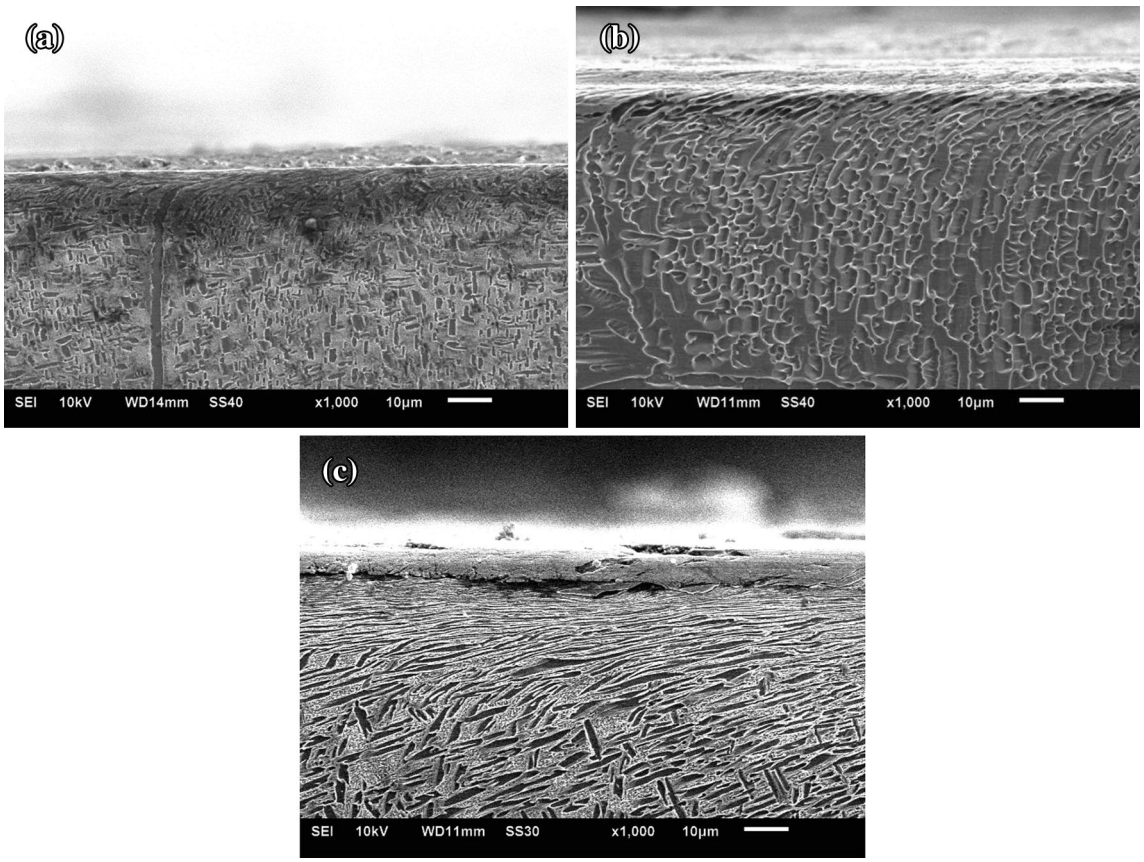

Fig. 5 Scanning electron micrograph of microstructure of: **a** unmodified LMD Ti–5Al–5Mo–5V–1Cr–1Fe alloy, **b** laser-nitrided and **c** thermal oxidation-treated LMD Ti–5Al–5Mo–5V–1Cr–1Fe alloy after sliding wear

observed on the unmodified and laser-nitrided LMD Ti–5Al–5Mo–5V–1Cr–1Fe alloy after dry sliding. For the thermal oxidation-treated LMD Ti–5Al–5Mo–5V–1Cr–1Fe alloy, plastic deformation was initiated in the subsurface beneath the surface oxide layer. A hardened zone in which lamellar α phase was distorted to accommodate plastic deformation was observed beneath the oxide/metal interface.

3.3 Wear rate, hardness and friction coefficient

The wear rates in terms of volume loss per unit of the total sliding distance ($mm^3\ m^{-1}$), friction coefficient and hardness of the unmodified, laser-nitrided and thermal oxidation-treated LMD Ti–5Al–5Mo–5V–1Cr–1Fe alloy are shown in Figs. 6, 7 and 8. It can be seen that surface treatment played an important role in determining the wear loss of the specimen. Under sliding against the bearing steel, the wear rate of the laser-nitrided LMD Ti–5Al–5Mo–5V–1Cr–1Fe alloy decreased 26 % as compared to the unmodified LMD specimens when their friction coefficients were similar. Hard dendritic TiN formed on the laser-nitrided LMD specimens is attributed to the

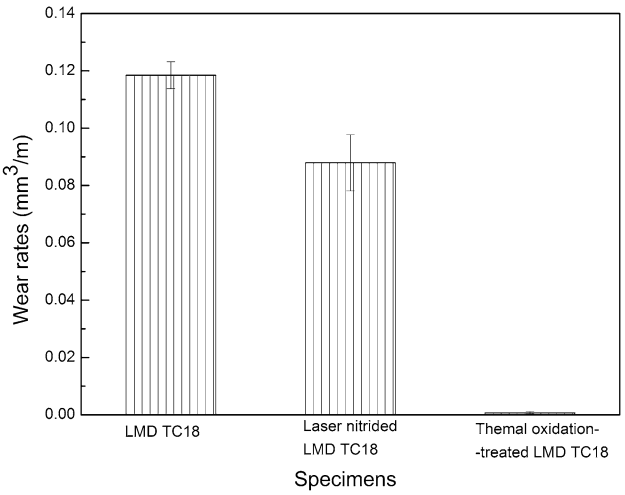

Fig. 6 Wear rate of unmodified, laser-nitrided and thermal oxidation-treated LMD Ti–5Al–5Mo–5V–1Cr–1Fe alloy

improvement on wear resistance. After laser nitriding, a 15 % increase in the hardness of LMD Ti–5Al–5Mo–5V–1Cr–1Fe alloy resulted in enhanced elastic contact that favored low adhesion between the contacting surfaces. The

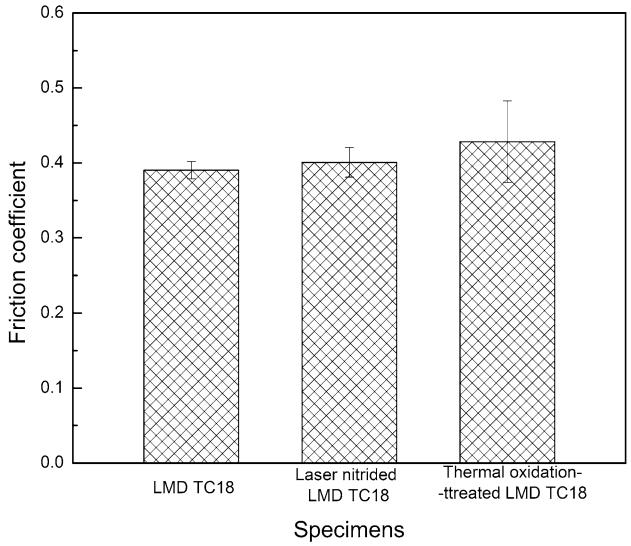

Fig. 7 Friction coefficient of unmodified, laser-nitrided and thermal oxidation-treated LMD Ti–5Al–5Mo–5V–1Cr–1Fe alloy

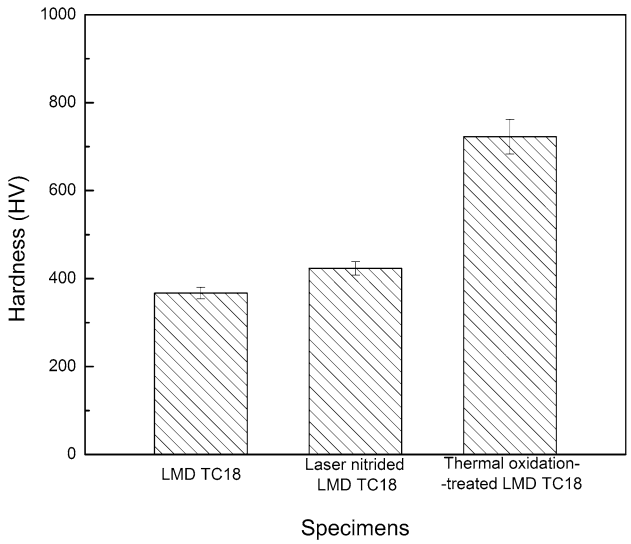

Fig. 8 Hardness of unmodified, laser-nitrided and thermal oxidation-treated LMD Ti–5Al–5Mo–5V–1Cr–1Fe alloy

wear rate of the thermal oxidation-treated LMD Ti–5Al–5Mo–5V–1Cr–1Fe alloy was <1 % of that of the unmodified LMD specimens. During thermal oxidation, solution of oxygen into α-Ti induced solid solution hardening that rendered the specimens double hardness. In the meantime, the rutile surface oxide layer formed on the thermally oxidized LMD specimen effectively impeded plastic deformation during dry sliding (see Fig. 5c) due to low shear strength coming from its particular crystallographic shear plane [12]. The low wear rate of the thermal oxidation-treated LMD Ti–5Al–5Mo–5V–1Cr–1Fe alloy is attributed to high elastic contact of the hardened diffusion zone as well as oxidation wear mechanisms operating between the contacting surfaces.

4 Conclusions

The unmodified LMD Ti–5Al–5Mo–5V–1Cr–1Fe alloy mainly comprised Ti in the form of α/β basket weave microstructure, and Ti, Ti_2N and TiN were observed on laser-nitrided LMD specimens. After thermal oxidation, a surface layer composed of rutile TiO_2 was formed on LMD specimens along with coarsening of α lath. Small flake-like wear debris coupled with a few remelted Ti–5Al–5Mo–5V–1Cr–1Fe alloy particles were formed on the laser-nitrided LMD specimens after sliding wear. The increase in hardness and wear resistance of the laser-nitrided LMD Ti–5Al–5Mo–5V–1Cr–1Fe alloy is attributed to hard dendritic TiN formed on the specimens. After thermal oxidation, the area of the wear scar was reduced significantly and powder-like fine debris originating from complex iron oxides was observed. The wear rate of the thermal oxidation-treated LMD Ti–5Al–5Mo–5V–1Cr–1Fe alloy was less than 1 % of that of the unmodified LMD specimens when hardness of the former was twice as much as the latter. The superior sliding wear resistance of the thermal oxidation-treated LMD specimens is attributed to the presence of the lubricious rutile oxide layer and hardened diffusion zone.

Acknowledgments The research work is sponsored by Beijing Higher Education Young Elite Teacher Project, the State Key Basic Research Program of China (Grant No. 2010CB731705) and the State Key Basic Research Program of China (Grant No. 2011CB606305).

References

1. R.J. He, H.M. Wang, Mater. Sci. Eng. A Struct. **1933**, 527 (2010)
2. E. Chlebus, B. Kuznicka, T. Kurzynowski, B. Dybala, Mater. Charact. **488**, 62 (2011)
3. C.M. Liu, X.J. Tian, H.B. Tang, H.M. Wang, J. Alloys Compd. **17**, 572 (2013)
4. L.L. Yu, X.N. Mao, P.S. Zhang, Y.Q. Zhao, S.C. Yuan, Rare Met. **21**, 24 (2005)
5. A.M. Mubarak, S.G.S. Raman, S.D. Pathak, R. Gnanamoorthy, Tribol. Int. **152**, 43 (2010)
6. P. Jiang, X.L. He, X.X. Li, L.G. Yu, H.M. Wang, Surf. Coat. Technol. **24**, 130 (2000)
7. Md OhidulAlam, A.S.M.A. Haseeb, Tribol. Int. **357**, 35 (2002)
8. S. Wang, Z.H. Liao, Y.H. Liu, W.Q. Liu, Surf. Coat. Technol. **64**, 252 (2014)
9. H. Guleryuz, H. Cimenoglu, Surf. Coat. Technol. **164**, 192 (2005)
10. S. Kumar, T.S.N.S. Narayanan, S.G.S. Raman, S.K. Seshadri, Mater. Chem. Phys. **337**, 119 (2010)
11. L. Liu, Y.J. Shangguan, H.B. Tang, H.M. Wang, Appl. Phys. A **1993**, 116 (2014)
12. A.R. Rastkar, T. Bell, Wear **1616**, 258 (2005)